Soft Matter

Cite this: *Soft Matter*, 2012, **8**, 5451

www.rsc.org/softmatter

PAPER

How does a supercoiled DNA chain pass through a small conical glass pore?

Qianjin Chen,[a] Shu Diao[a] and Chi Wu†*[ab]

Received 16th February 2012, Accepted 7th March 2012
DOI: 10.1039/c2sm25346a

We investigated the captioned question by a resistive pulse technique, in which a constant electrical potential was applied inside and outside of a conical glass capillary with its tip opening diameter (d) down to ~10 nm. The insertion of a chain segment into the tip decreases the current (I_p). Our studies on transport dynamics of individual supercoiled DNA chains through such a tip with different openings at various potentials (V) reveal that when $d \approx 35$ nm, they can pass through the conical glass capillary without much stretching; namely, the current pulse has a typical triangle shape and its half-height duration time ($\Delta t_{d,1/2}$) decreases, but its occurring frequency (f) increases exponentially, as V increases. For a smaller tip opening ($d \approx 14$ nm), we found that f strangely increases and then decreases with increasing V. In addition, the current pulse is significantly skewed with a long tail and its minimum occurs when $V \approx 200$ mV. Typically, each current pulse is composed of four steps as follows: (1) I_p sharply decreases from its baseline (I_o) when a DNA chain approaches the tip opening and inserts a segment to block the pore; (2) the inserted segment is stretched under the electric field gradient so that the pore is less blocked, resulting in a slight current increase; (3) then I_p slightly decreases once more, indicating that the pulling of the inserted segment is faster than the relaxation (unwinding) of the rest of the chain outside so that it clogs at the tip entrance; and (4) I_p gradually increases and finally returns to I_o because more and more segments are gradually pulled in by the electrical field until the entire chain slips through the conical glass capillary. These steps can be well explained in terms of a big difference between times of pulling the first segment inside the tip and relaxing the rest of the segments outside.

Introduction

The translocation of individual macromolecular chains through a small pore ($d \approx 10$ nm) has attracted much interest in recent years. The charged chains, such as synthetic polyelectrolytes and DNA, are usually driven by an electrical force. In these experiments, a membrane with a biological[1–16] or synthetic[17–32] pore is placed between two electrolyte solutions and a constant transmembrane electric potential is applied. The passage of a charged chain or particle through a small pore by an electric force leads to a transient current decrease because of its excluded volume. With fast electronics and sensitive detection, each translocation event can be recorded with a higher time resolution so that its structure and translocation dynamics could be evaluated. In the past years, such a method has been tried to discriminate bases of nucleic-acid,[1–3] probe local structure of DNA,[4–9,17–24] RNA[10] and proteins;[11,12,25–27] and measure forces required to unzip a nucleic acid[13,28,29] or rupture a DNA–protein complex.[30] Harrell *et al.*[19] used a double-stranded plasmid DNA (6.6 kbp) and a conical polymer pore with a tip opening with a diameter of $d = 40$ nm to study the DNA translocation but only observed short-duration events due to collisions or "bumping", presumably because the ds-pDNA is a supercoiled circular DNA, and hence has much less flexibility than conventional ds-DNA.

On the other hand, the translocation of neutral macromolecules through a small pore has to be driven by a hydrodynamic force, such as an elongation flow.[33,34] In the past few years, a combination of a commercially available membrane with 20 nm pores and laser light scattering (LLS) was used to study the ultra-filtration of: (1) flexible linear polystyrene chains, confirming the first order coil-to-stretch transition;[35,36] (2) star polystyrene chains, developing a novel method to separate polymer chains by their topologies instead of size;[37,38] and (3) spherical core–shell micelles made of block copolymers, unearthing the interaction strength (down to ~10 fN) of the insoluble blocks inside the core.[39,40] Recently, a scaling argument and a first principle calculation were developed to consider the draining of the chain confined inside a cylindrical pore,[41,42] which successfully account for much smaller measured critical flow rates. However, these experiments only measured a collective property, *i.e.*, the critical flow rate, and how a macromolecular chain changes its conformation through a small pore (<20 nm) remains unaddressed, presumably due to some experimental difficulties. Recently, the translocation of DNA in very small

[a]*Department of Chemistry, The Chinese University of Hong Kong, Shatin, N.T., Hong Kong. E-mail: chiwu@cuhk.edu.hk*
[b]*The Hefei National laboratory of Physical Science at Microscale, Department of Chemical Physics, The University of Science and Technology of China, Hefei, Anhui 230026, China*
† The Hong Kong address should be used for all correspondence.

solid-state nanopores were reported,[28,43,44] suggesting that the translocation dynamics were very different from that in a large pore. Such complexity is attributed to DNA–pore interactions during translocation.

The small pores made of different proteins have some unique properties developed through genetic engineering and chemical modification.[6] The limitations are their fixed pore sizes and mechanical fragility of the lipid bi-layer in which they are embedded. Therefore, pores made of rigid and strong materials gradually gain more attention for single biopolymer analysis. Instead of using solid Si_3N_4 and a focused-ion-beam, requiring expensive instruments,[31,45] one can also fabricate a conical glass capillary with its tip opening as small as 10 nm in diameter by a simple sealing–polishing–etching procedure with no special equipment but some patience and skills.[32] In the current study, we fabricated conical glass capillaries with a tip opening down to 14 nm to study the translocation of DNA. Supercoiled plasmid DNA instead of conventional linear ds-DNA is chosen because the supercoiled structure has higher chain rigidity, enabling the single chain coil-to-stretch transition during translocation in a small pore to be more easily observed.[46] Our results show the distinct transport dynamics with different pore sizes. For the large pore, the expected dynamics, *i.e.*, the monotonic dependence of the event duration time, blockade current and frequency, were observed, but for the small pore, we observed that the translocation of most of the DNA chains took four steps, which can be correlated to the change of chain conformation and the relative difference between the chain relaxation time and the pulling time under an applied electric field.

Experimental section

Materials

The plasmid LUNIG-Luc of 10 kbp was transformed into *E. coli* XL-1 Blue bacteria, cultured and purified using a Plasmid Extraction Maxi Kit (QIAGEN, Cat#12162).[47] The purity and quantity of the obtained plasmid were assessed by agarose gel electrophoresis and ultraviolet absorbance. The typical DNA concentration of the stock solution in Tris buffer (pH 7.4) was 1.4 mg mL^{-1}. The gel electrophoresis shows that freshly extracted plasmid DNA mainly has a supercoiled chain conformation.

Fabrication of a small conical glass capillary

Borosilicate capillaries (1.5 mm o.d. and 0.8 mm i.d.) were purchased from A-M System, Inc. Before use, the capillary was washed with ethanol and D.I. water, followed by drying in nitrogen air. The end of such a cleaned tube was put in the flame at ~700 °C. After softening, the tip was pulled with the assistance of tweezers, and cut in the middle, followed by heating the very end of the cross-section. The left inset in Fig. 1 shows such a conical glass capillary with its end still sealed. To expose its cavity, we polished its sealed end with a fine sand paper and stopped just before exposing its cavity, judged by an optical microscope. The capillary was then immersed into a glass etchant (10% HF : 0.83 M NH_4F : 3 M HNO_3 = 1 : 3 : 1, volume ratio) with its inner cavity filled with dust-free 1.0 M KCl solution. The etching process was *in situ* monitored by measuring the conductance across the membrane, as shown in Fig. 1. The

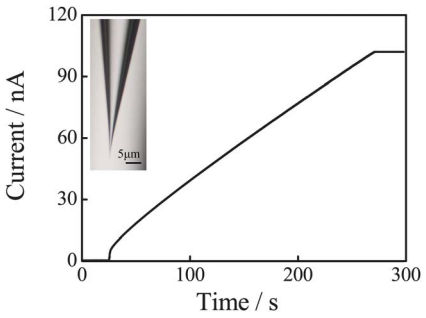

Fig. 1 Etching time dependence of conductance of a typical conical glass capillary, where 50 mV is applied between the inside and outside of capillary. The inset is an optical microscopy image of a capillary before etching.

gradual increase of the current indicates that the cavity enclosed in the tip is ultimately perforated to form a small opening. Once etched through a proper opening, the pipette tip was washed with an excessive amount of water to neutralize the surface. The final diameter of each conical glass capillary was determined by electrical conductance in 1.0 M KCl solution, as shown in Fig. 2A and confirmed by scanning electron microscopy. The estimated half-angle of a typical conical cavity is ~2.5°.

Current-pulse measurements

A HP PC with a National Instruments (NI) PCI-6251 data acquisition board and BNC-2090 was used for data acquisition. A Dagan Chem-Clamp voltammeter/amperometer was used as a potentiostat. Current–time (*i–t*) curves were recorded using an in-house virtual instrument written in NI Labview 8.5. The current was monitored with a 300 kHz sampling rate and a 10 kHz filter. All the experiments were done inside a home-built Faraday cage at room temperature (23.0 ± 0.5 °C). The current pulse amplitudes and durations were analyzed using a commercial Igor Pro 6.02 and QuB software package.

Results and discussion

Fig. 2B shows typical *I–V* characteristics of three conical glass capillaries with different conductances. For comparison, we also

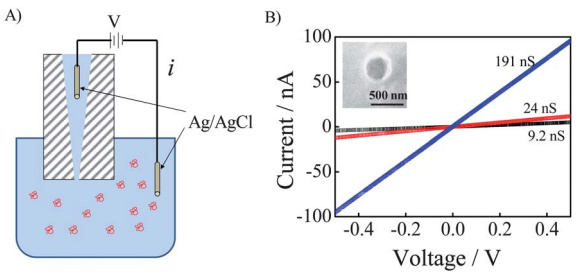

Fig. 2 (A) Experimental setup for single-molecule measurement with a conical glass capillary, where both the inside and outside of capillary were filled with buffer solution (1.0 M KCl, 10 mM Tris, pH 7.4) and P-DNA was only added to the outside and (B) typical *I–V* characterization curve for capillaries with different tip openings, where each conductance is marked and the inset shows an SEM image of a conical glass capillary with a conductance of 191 nS.

characterized different conical glass capillaries by SEM and established a relationship between their tip diameters and conductance. We adapted the methods proposed and used by White and his coworkers:[48,49]

$$R_p = \frac{1}{\kappa a_p}\left(\frac{1}{\pi \tan\theta} + \frac{1}{4}\right) \quad (1)$$

where R_p is the resistance, a_p is the small orifice radius, κ is the conductivity of the solution (10.5 Ω^{-1} m^{-1} for 1.0 M KCl solution), and θ is the conical half-angle measured by an optical microscope. For a conical glass capillary with a conductance of 191 nS, the radius estimated on the basis of eqn (1) is 137 nm with $\theta = 2.5°$, agreeing well with that (147 nm) measured by SEM. Hereafter, listed diameters (d) of the capillaries used are estimated from conductance. In the current study, we mainly used two capillaries with d = 14 nm and 35 nm, respectively. To eliminate air bubbles, we filled the capillary with 1.0 M KCl, 10 mM Tris buffer (with 1 mM EDTA, pH 7.4) and vacuumed it using an oil pump for ~5 s. The capillary is then immersed in the same electrolyte solution. Before adding DNA into the outside solution, the current trace was recorded as the baseline (I_o). After adding 5 μL of 1.4 mg mL^{-1} plasmid DNA solution into 990 μL of buffer, we slightly mixed the solution with the pipette tip. The final DNA molar concentration was ~1.06 nM. Within a few minutes after DNA was added, many current peaks were observed at different applied voltages (V), as shown in Fig. 3A and C for d = 14 nm and Fig. 3B and D for d = 35 nm.

Fig. 3E and F show typical highly time-resolved translocation events. Each of them contains different stages described as follows. The initial sharp decrease of the current in each pulse can be attributed to the blockade of the tip from outside by a coiled DNA chain. The shapes of event peaks for different tip openings are obviously different. For d = 14 nm, the peak shape is quite complicated, with multiple levels of current. The majority (83%) of events are type A with two downward sub-peaks, while B and C are minority with only one peak.

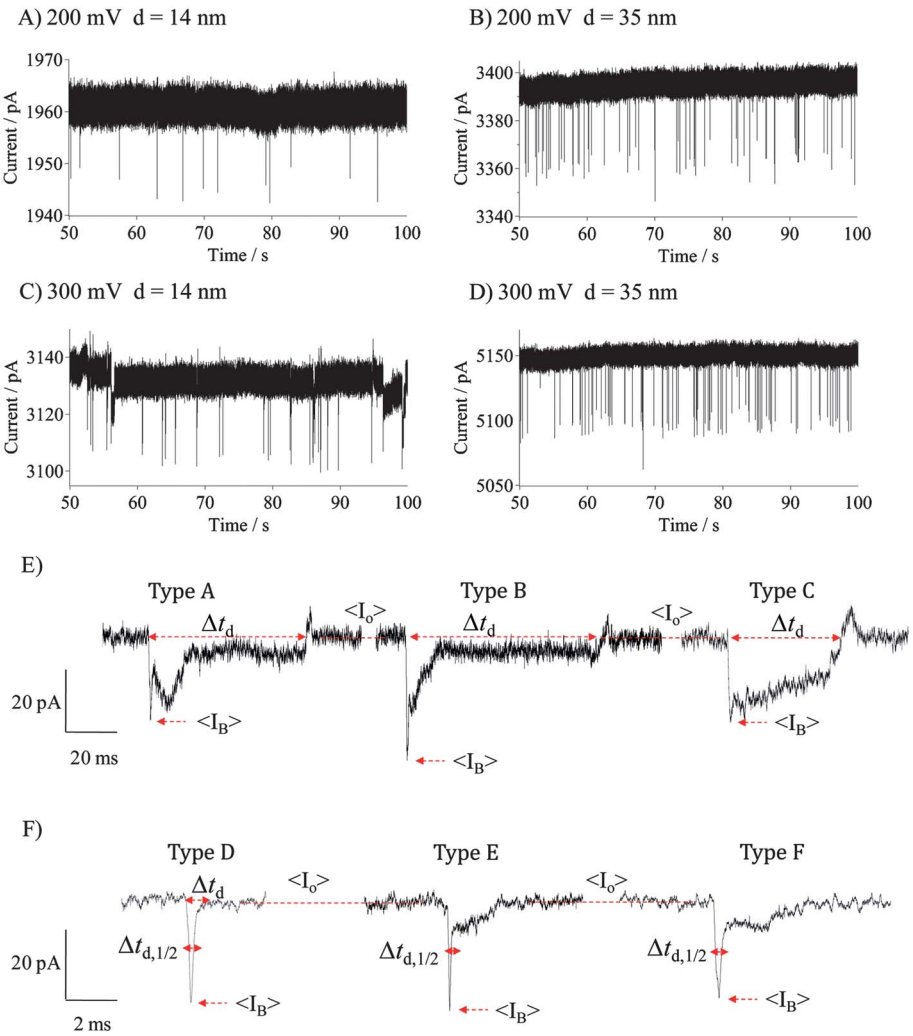

Fig. 3 Representative current traces after adding DNA into solution for two different tip openings and at different applied voltages, where each downward pulse reflects a single-molecule event (translocation through conical glass capillary), where DNA concentration is 1.06 nM in buffer solution 1.0 M KCl, 10 mM Tris, pH 7.4. The lower panels display zoom-ins for some typical events, where types E and F are from d = 14 and 35 nm at 300 mV, respectively. $\langle I_o \rangle$ and $\langle I_B \rangle$ indicate current levels for open and blockade states, respectively; Δt_d represents duration time but for events with a triangle pulse in F the half-height duration time $\Delta t_{d,1/2}$ is used to reduce possible measurement errors.

Note that for type A events, the minimum current level usually occurs at the first downward peak, as shown in Fig. 3E, and it occurs with a relatively lower percentage at lower voltages. For $d = 35$ nm, type D often occurs with a triangle shape, while types E and F occur only occasionally (<5% of the total population) with a much longer tail. The event blockade current is defined as $\langle \Delta I \rangle = \langle I_o \rangle - \langle I_B \rangle$, shown in Fig. 3. For events with a triangle shape, we define the half-height width $\Delta t_{d,1/2}$ instead of Δt_d because there is a large error in its measured peak duration time. The duration time and blockade current for each event are manually measured based on the current traces at different voltages for different pore sizes. The current traces in Fig. 3A–D are similar to those previously recorded by using silica nanochannels,[50] small polycarbonate conical pores[19] or quartz capillaries,[22,51] evidencing that these current pulses are indeed related to the translocation of individual DNA chains through our current conical glass capillaries.

Fig. 4 shows some typical statistics of the events with different applied voltages (V) and tip openings (d). As expected, the mean blockade current ($\langle \Delta I \rangle$) increases with V in spite of different tip openings. For a given V, the event durations for $d = 14$ nm are much longer than those for $d = 35$ nm. In Fig. 4B and D, a shorter duration is often correlated to a higher blockade current. Such correlation indicates that each DNA chain remains in its less stretched coiled state during its translocation, described by $\langle \Delta I \rangle \Delta t_d = \langle \Delta I_{str} \rangle \Delta t_{d,str}$, where $\langle \Delta I \rangle$ and Δt_d are respectively the mean blockade current and duration time; the subscript "str" denotes a fully stretched DNA chain. The persistence length (a measure of chain stiffness) of double-stranded DNA chain is ~33 nm in 1 M salt solution[52] and that of plasmid DNA chains should be even longer. Therefore, our currently used supercoiled plasmid DNA chains would have to be partially stretched before passing through the 14 nm tip and would result in a flat bottom in each current pulse with a step-like shape. However, no such pulse was observed, which is probably because our conical capillary has a large sensing volume inside.

For $d = 35$ nm, we can use the Gaussian fitting to obtain the most probable translocation duration time ($\Delta t_{d,1/2}$) from the duration time distributions in Fig. 4B and D; namely, $\Delta t_{d,1/2} =$ 225 and 272 μs, respectively, at $V = 300$ and 200 mV, increasing as the voltage decreases. While for the small tip opening ($d =$ 14 nm), the duration time distribution is much broader. The most probable duration time is much longer, in ms instead of in μs, and increases ~15 times from 4 ms to 62 ms, when the applied voltage increases from 200 mV to 300 mV. Further increase of the applied voltage makes the tip act as a "gate"; namely the measured current drops and reaches a noise level with no further detectable events, indicating that the tip opening is completely blocked and stuck by one DNA chain. A similar observation was reported before.[43] However, our observed single histogram peak in Fig. 4 indicates that there should be no obvious binding of DNA on all the capillaries at the applied voltages.

Fig. 5A shows that the voltage dependence of the average duration time can be described as an exponential function, instead of an inverse one between duration time and electric force, because each DNA chain has to be stretched in the translocation, which involves an extra energy barrier.[25,53] For $d = 35$ nm, we have $V_c = 478$ mV and $z = (k_B T)/(eV_c) = 0.054$,

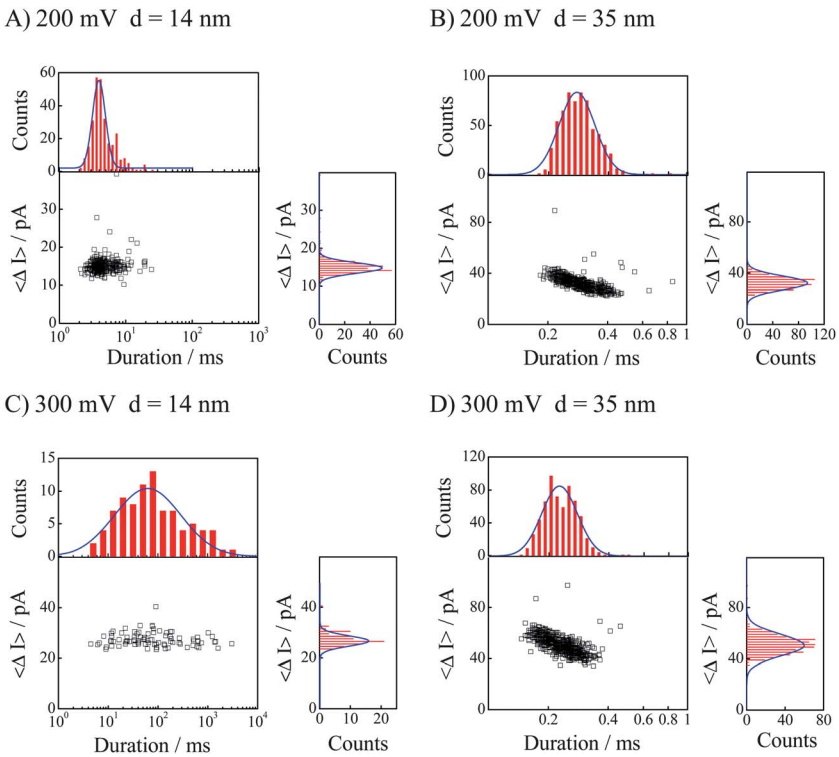

Fig. 4 Statistics of events of translocation of supercoiled pDNA chains through conical glass capillaries with different openings and at different applied voltages, where each data point represents one translocation event, where (A), (B), (C) and (D) are from 288, 620, 93 and 615 events, respectively.

deduced from the voltage relationship for a capillary. Note that such a value (the effective charge of a DNA chain inside our conical glass capillary) is much smaller than those reported for ss-DNA[7,54] and proteins[11] using a small protein pore, presumably due the their geometric difference. For $d = 14$ nm, Δt_d shows an expected decrease as V increases from 120 mV to 200 mV. However, further increase of V to 300 mV unexpectedly increases Δt_d.

In the current setup, our conical glass capillary was treated with acid during its fabrication so that its surface is cationic in a KCl solution. Under an applied voltage, cations flow out of the tip but anions and DNA flow in. The opposite flows could slow down and even hinder the penetration of a long DNA chain into the pore.[6,55,56] As the applied voltage increases, such an effect becomes more evident. However, the Debye length in 1.0 M KCl is only ~0.3 nm, much smaller than our tip opening. The questions are whether such an effect alone could make the duration time 15 times longer when the voltage increases only from 200 mV to 300 mV and why there is a minimum, rather than a monotonic increase. We will discuss this point later.

Fig. 5B shows that for $d = 35$ nm, $\langle \Delta I \rangle / \langle \Delta I \rangle_o$ decreases as V increases. Such a tendency was also observed for single-stranded homopolymers passing through a 10 nm silicon nitride nanopore.[44] It suggests that the relative volume occupied by each DNA chain inside the conical capillary at a higher voltage is smaller, presumably because it is more stretched with an increasing force gradient and becomes more draining. Quantitatively, the normalized blockade current ($\langle \Delta I \rangle / \langle \Delta I \rangle_o$) is compared to its theoretical value, the volume ratio of a DNA chain to the sensing part of the conical capillary, V_{DNA}/V_{pore}. Unlike a polystyrene particle or an entirely folded protein, the coiled DNA chain in the presence of a large amount of salts should be draining and permeable by counter ions. Assuming that the DNA chain inside the capillary fills up the conical volume, *i.e.*, $V_{DNA}/V_{pore} = 1$, as schematically shown in Fig. 6A, we can estimate the permeation factor (p) to be ~99% from $\langle \Delta I \rangle / \langle \Delta I \rangle_o = (1 - p) V_{DNA}/V_{pore}$.

On the other hand, considering that each DNA chain is pulled and elongated as a cylinder under the electric field gradient after entering the tip opening ($d = 35$ nm), as schematically shown in Fig. 6B. Assuming that there is no change in its hydrodynamic volume, we can estimate its stretched length (L) to be $\sim 3 \times 10^3$ nm from $\pi(35/2)^2 L = 4\pi \langle R_h \rangle^3/3$, where $\langle R_h \rangle$ (~90 nm) is the effective hydrodynamic radius of p-DNA chains in 1.0 M KCl, measured by dynamic LLS. Using this estimated L, we estimated the conical volume ($V_{pore} = 5.3 \times 10^7$ nm^3) reached by the inserted chain. A comparison of the measured $\langle \Delta I \rangle / \langle \Delta I \rangle_o$ and the estimated V_{DNA}/V_{pore} (= 5.4%) leads to $p = 85\%$. Physically, Fig. 6A should be more reasonable.

For $d = 14$ nm, $\langle \Delta I \rangle / \langle \Delta I \rangle_o$ depends on voltage in a very different way. Namely, it first slightly decreases and then increases. Since the persistence length of DNA is much longer than d, the chain segment at the tip opening should be fully stretched. The change of $\langle \Delta I \rangle / \langle \Delta I \rangle_o$ with voltage involves either the conformation change inside the pore or the blockage of the chain just outside the tip or both. The possible interaction between the pore and DNA could not be ignored, especially when the pore is very small. The increase of $\langle \Delta I \rangle / \langle \Delta I \rangle_o$ with voltage was observed before for both ds-DNA and ds-RNA in smaller pores (3–10 nm),[43,44] which was attributed to the enhanced interaction at higher voltages. We are able to use it to explain our results from the small pore in the high voltage range, but not for our results obtained in the low voltage range.

Fig. 5C shows that the event frequency (f) as a function of the applied voltage (V) can be generally described by a van't Hoff–Arrhenius law: $f = f_o \exp(|V|/V_0)$, where $f_o \propto \exp(-U^*/kT)$, the event frequency with no applied voltage, U^* is the activation

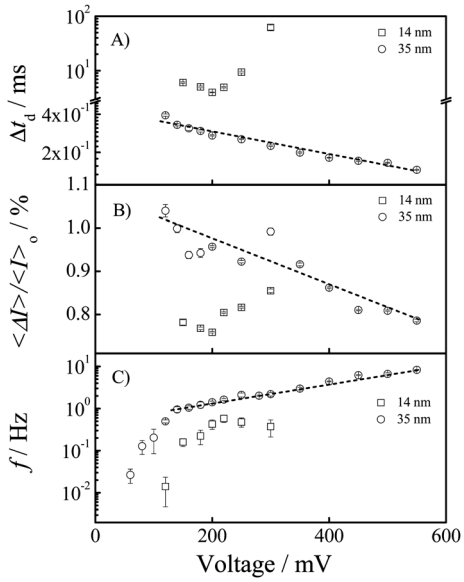

Fig. 5 Voltage dependence of (A) duration time (Δt_d for $d = 14$ nm and $\Delta t_{d,1/2}$ for $d = 35$ nm), where we used $\Delta t_{d,1/2} = A\exp(|V|/V_c)$ to fit data and found that $A = 0.44 \pm 0.03$ ms and $V_c = 478 \pm 31$ mV; (B) normalized blockade current ($\langle \Delta I \rangle / \langle \Delta I \rangle_o$); and (C) event occurring frequency (f), where the dashed line in the high voltage range describes a fitting of $f = f_0 \exp(|V|/V_0)$ with $f_0 = 0.47 \pm 0.03$ Hz and $V_0 = 186 \pm 7$ mV, where each point in (A) and (B) were obtained from 400–800 events for $d = 35$ nm, 100–400 events for $d = 14$ nm and each point in (C) was obtained from 500–2000 events for $d = 35$ nm and 100–400 events for $d = 14$ nm, respectively.

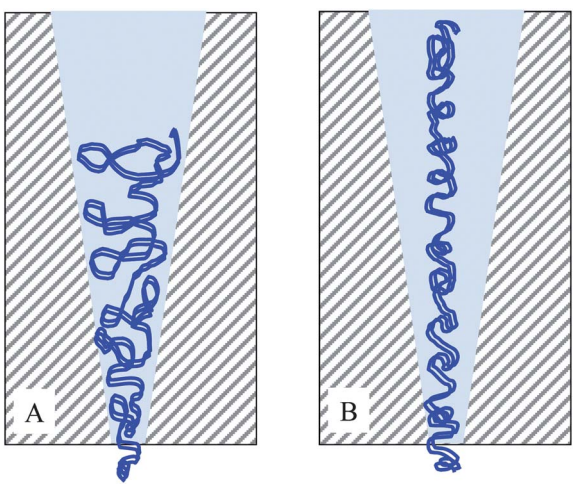

Fig. 6 Schematic of a DNA chain pulled inside a small conical glass capillary.

energy, and $|V|/V_0$ ($= ze|V|/kT$) is a barrier reduction factor due to the applied voltage with z, the magnitude of the total effective number of elementary charges (e) on a chain.[7] Note that z is related to several effects: the access resistance, the charge distribution and the chain conformation at the pore entrance. The potential V_0 corresponds to the minimum voltage required to overcome the thermal energy as well as possible electrostatic interaction between the chain and the pore. For $d = 35$ nm, the data in the high voltage range are well described by $f = f_o \exp(|V|/V_o)$ with $f_o = 0.47 \pm 0.03$ Hz (at $c = 1.06$ nM) and $V_o = 186 \pm 7$ mV. The estimated value of $z = 0.14$ is quite low, as discussed in the analysis of duration time. Recently, the force exerted on a single DNA chain inside a nano-capillary was measured by a combination of nano-pores and optical tweezers,[51] which is much weaker than expected. For $d = 14$ nm, f anomalously increases in the voltage range 120–220 mV, but then decreases when V further increases in the range 220–300 mV.

For a given DNA concentration, the capture probability (event frequency) through the tip is determined by the pulling force and the chain diffusion. For $d = 35$ nm, the event duration time is typically less than 1 ms, much shorter than the inter-event interval time, implying that f is mainly controlled by diffusion. Even at a voltage as high as 550 mV, where the inter-event time is ~95 ms estimated from the Gaussian fitting, f is still not saturated to a constant, indicating that the diffusion time of a DNA chain towards the tip is shorter. On the other hand, even for $d = 14$ nm, the event duration time in the low voltage range is still shorter than the diffusion time so that f should still be controlled by diffusion. Only when the event duration time is close to or longer than the diffusion time, f would become controlled by the translocation. Therefore, in the voltage range 220–300 mV, longer dwell time results in less efficient translocation, *i.e.*, the lower event frequency.

As expected, for a relatively larger tip opening, individual DNA chains can pass through it without a significant alternation of its coiled conformation, while for a small tip opening, each DNA chain has to be stretched and pulled through it. It can be visualized that pulling the first segment of a DNA chain inside the tip will create a tension on the rest of the segments outside. When a lower voltage is used to slowly pull one segment into the tip, the rest of the segments outside have a sufficient time to relax and follow the first pulled segment without creating much tension so that the DNA translocation is similar to that for a relatively larger tip opening. However, when a higher voltage is applied, a DNA chain is fast-pushed towards the tip and one segment is quickly pulled into the tip opening and stretched but the rest of the segment outside might have no time to relax so that they are interlocked into each other and stuck at outside of the tip entrance. Using such a difference in the pulling and relaxation times, we are able to explain some complicated current profiles and those anomalous voltage dependences of the normalized blockade current, duration time and event frequency when a glass conical capillary with a small tip opening is used. For example, the long duration time at higher applied voltages is related to the slow release of the interlocked segments; and the strange lower event frequency at 300 mV is attributed to the complete blockage of the tip opening.

Fig. 7 schematically summarises our above discussion based on the shapes of the current pulses in Fig. 3E. In Step I, a DNA chain driven by the electric force moves towards the entrance of the tip with a diameter much smaller than its hydrodynamic size. When it collides with the tip, one segment is sucked in and blocks the tip opening so that the effective opening is dramatically reduced, resulting in a current drop, the first downward peak. In Step II, the electric force pulls and stretches the inserted segment, which actually reduces the blockade of the tip opening and leads to a slight increase of the current, as shown in Fig. 3E. Note that in order to pull the rest of the chain into the conical capillary, the inserted segment has to be fully stretched before it exerts a force on the rest of the chain stuck at the outside of the tip. As soon as the rest of the chain is pulled, the segments outside of the tip would be forced to come together if there was no sufficient time for them to relax (slide) from each other into the tip opening, which would increase the chain density outside, reduce the counter ion draining and result in a slight decrease of the current, as shown in Step III. Further, Step IV shows that under a constant and sufficiently strong pulling force, the interlocked chain segments outside are gradually relaxed to reduce the tension so that they are eventually pulled inside the tip in a one-by-one fashion, leading to a slow increase of the current and final recovery of the current to its initial value (I_o) when the entire DNA chain is pulled through the tip opening.

Quantitatively, we are able to measure an average duration time (τ_S) required to stretch the first segment inserted into the tip opening in the second step for type A events, as shown in Fig. 3E namely, $\tau_S = 484 \pm 16$ μs at 300 mV when the Gaussian fitting is used. On the other hand, we can also estimate the time needed for the rest of the chain outside to relax from the relaxation time (τ_R) of the first Rouse–Zimm normal mode for a DNA chain,[57,58]

$$\tau_R = \frac{1}{(3\pi)^{1/2}} \frac{\eta_s b^3 N^{3/2}}{k_B T} = \frac{1}{(3\pi)^{1/2}} \frac{\eta_s R_F^3}{k_B T} \quad (2)$$

where b and N are the Kuhn length and number of Kuhn segments per chain and η_s and R_F are the solvent viscosity and the average chain end-to-end distance, respectively. For an ideal chain, $R_F^2 = b^2 N$ and $R_G^2 = b^2 N/6$ so that $\tau_R \approx 7.3$ ms with

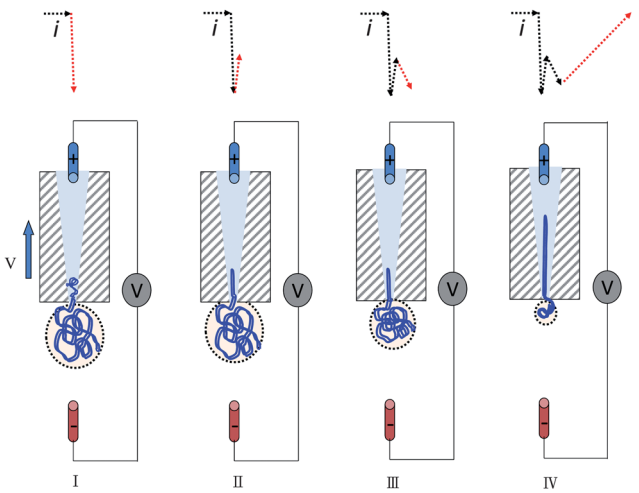

Fig. 7 Schematic of translocation dynamics of a supercoiled plasmid DNA chain through a small conical glass capillary at a high applied voltage and their corresponding current response based on Fig. 3E.

$R_G \approx 190$ nm measured in 1.0 M KCl solution by static LLS. However, considering that the segments outside are entangled with each other, we should estimate the relaxation time from the reptation limit by[57,58]

$$\tau_R \approx \frac{b^2 N^3 \phi^{3/2}}{D} \approx \frac{b^3 N^3 \phi^{3/2}}{Db} \approx \frac{6\pi\eta_s L_c^3 \phi^{3/2}}{k_B T} \quad (3)$$

where L_c is the contour length of DNA and ϕ is the chain density in its occupied volume. For a 10 kbp plasmid DNA, $L_c \approx 7.5$ μm and $\phi \approx 0.36\%$ estimated from $\phi = M_w/(N_A \times 4\pi/3 \times R_h^3)$ with M_w and R_h being the weight-average molar mass and average hydrodynamic radius of DNA, respectively. In this way, $\tau_R \approx$ 370 ms, much longer than that calculated from the longest Rouse–Zimm relaxation. In either case, $\tau_R > \tau_S$ so that the rest of the chain is stuck onto the tip opening when the first inserted segment is quickly pulled. Such relaxation of a DNA chain was previously visualized by fluorescence microscopy, in which one chain end was attached to a bead that was manipulated with optical tweezers and the other end was stretched by a hydrodynamic force (an elongation flow).[59] The measured relaxation time (few seconds) was longer than the estimated Zimm relaxation time. Moreover, the measured force of stretching a DNA chain was in the pN range,[60,61] fairly close to that for DNA in nano-capillaries.[51]

One tentative reader might find that Fig. 3E shows an overshoot of the current at the end of Step IV for different types of the events before the current returns to its corresponding initial value (I_o). It should be emphasized that this is not an electronic signal overshoot because the current traces have no such feature when a tip with a larger opening is used. Such an overshoot is actually attributed to charges on DNA; namely, when a DNA chain moves from the tip upwards, its carried charges move in the same direction, which should slightly increase the measured current in comparison with I_o in the pure electrolyte solution without DNA. Such a current enhancement for the biopolymer translocation was also observed before.[62,63]

Conclusion

The studies of translocation of supercoiled 10 kbp plasmid DNA through a small conical glass capillary with different tip openings and at different applied voltages have unearthed its detailed chain dynamics at the tip entrance. For the tip with a relatively large opening ($d = 35$ nm), this is not surprising; namely, the translocation frequency increases, but the half-height duration time decreases exponentially as the applied voltage increases; and the normalized blockade current is less affected by the voltage, agreeing well with the electrophoresis theory. When the tip opening ($d = 14$ nm) is much smaller than the size of a coiled plasmid DNA chain, it adopts a very different translocation dynamics through the conical glass capillary, depending on the applied voltage. Our results reveal that there exist two different times; namely, one is the time (τ_S) needed to stretch the first chain segment inserted into the tip opening by the electrical pulling force; and the other is the time (τ_R) required for the rest of the chain segments outside the tip to relax under such a pulling so that they can slip through the tip opening in a one-by-one fashion. Quantitatively, τ_S estimated from Step II in type A current pulse is 484 ± 16 μs at 300 mV, while τ_R ranges from 7.3 to 370 ms, depending on whether we use the relaxation time of the first Rouse–Zimm normal mode or the time for a chain to reptate from its entangled surrounding. When $\tau_S \gg \tau_R$ (a relatively larger tip opening or a relatively lower applied voltage), each chain can deform and pass through the glass capillary without blocking the tip opening because each segment has a sufficient time to relax and follow the pulling force. On the other hand, when $\tau_S \ll \tau_R$ (a smaller tip opening or a higher applied voltage), quickly stretching the first segment inserted inside the tip opening exerts a force on the rest of the chain outside and creates a tension but the chain does not have sufficient time to relax. Therefore, they are interlocked with each other and stuck onto the tip with a relatively more compact and less draining conformation, slowing down its translocation through the tip opening. To the best of our knowledge, this is the first explanation detailed for how multiple levels of the current blockade correspond to the chain conformational change, different from those previously reported for the translocation of DNA or RNA through a protein channel or a small solid-state cylindrical pore. Using these two different time scales, we are able to satisfactorily explain the translocation dynamics and those complicated shapes of the current pulses measured in a small pore. Our current study also shows that conical glass capillaries can be easily fabricated and effectively used in the resistive-pulse technique to detect the translocation of individual macromolecular chains.

Acknowledgements

The financial support of the National Natural Scientific Foundation of China Projects (50773077 and 20934005) and the Hong Kong Special Administration Region Earmarked Projects (CUHK4046/08P, 2160365; CUHK4039/08P, 2160361; CUHK4042/09P, 2160396; and CUHK4042/10P, 2130241; 2060405) is gratefully acknowledged. The authors thank Professor Bo Zheng for assisting us in optical microscopic measurements.

References and notes

1 N. Ashkenasy, J. Sánchez-Quesada, H. Bayley and M. R. Ghadiri, *Angew. Chem., Int. Ed.*, 2005, **44**, 1401–1404.
2 A. Meller, L. Nivon, E. Brandin, J. Golovchenko and D. Branton, *Proc. Natl. Acad. Sci. U. S. A.*, 2000, **97**, 1079–1084.
3 D. Stoddart, A. J. Heron, E. Mikhailova, G. Maglia and H. Bayley, *Proc. Natl. Acad. Sci. U. S. A.*, 2009, **106**, 7702–7707.
4 J. J. Kasianowicz, E. Brandin, D. Branton and D. W. Deamer, *Proc. Natl. Acad. Sci. U. S. A.*, 1996, **93**, 13770–13773.
5 D. K. Lathrop, E. N. Ervin, G. A. Barrall, M. G. Keehan, R. Kawano, M. A. Krupka, H. S. White and A. H. Hibbs, *J. Am. Chem. Soc.*, 2010, **132**, 1878–1885.
6 G. Maglia, M. R. Restrepo, E. Mikhailova and H. Bayley, *Proc. Natl. Acad. Sci. U. S. A.*, 2008, **105**, 19720–19725.
7 A. Meller, L. Nivon and D. Branton, *Phys. Rev. Lett.*, 2001, **86**, 3435–3438.
8 R. F. Purnell and J. J. Schmidt, *ACS Nano*, 2009, **3**, 2533–2538.
9 A. E. P. Schibel, N. An, Q. Jin, A. M. Fleming, C. J. Burrows and H. S. White, *J. Am. Chem. Soc.*, 2010, **132**, 17992–17995.
10 T. Z. Butler, J. H. Gundlach and M. A. Troll, *Biophys. J.*, 2006, **90**, 190–199.
11 M. Pastoriza-Gallego, L. Rabah, G. Gibrat, B. Thiebot, F. G. van der Goot, L. Auvray, J.-M. Betton and J. Pelta, *J. Am. Chem. Soc.*, 2011, **133**, 2923–2931.

12 H.-Y. Wang, Y.-L. Ying, Y. Li, H.-B. Kraatz and Y.-T. Long, *Anal. Chem.*, 2011, **83**, 1746–1752.
13 A. F. Sauer-Budge, J. A. Nyamwanda, D. K. Lubensky and D. Branton, *Phys. Rev. Lett.*, 2003, **90**, 238101.
14 Q. Chen, J. Liu, A. E. P. Schibel, H. S. White and C. Wu, *Macromolecules*, 2010, **43**, 10594–10599.
15 R. J. White, E. N. Ervin, T. Yang, X. Chen, S. Daniel, P. S. Cremer and H. S. White, *J. Am. Chem. Soc.*, 2007, **129**, 11766–11775.
16 A. Aksimentiev, *Nanoscale*, 2010, **2**, 468–483.
17 P. Chen, J. Gu, E. Brandin, Y.-R. Kim, Q. Wang and D. Branton, *Nano Lett.*, 2004, **4**, 2293–2298.
18 D. Fologea, M. Gershow, B. Ledden, D. S. McNabb, J. A. Golovchenko and J. Li, *Nano Lett.*, 2005, **5**, 1905–1909.
19 C. C. Harrell, Y. Choi, L. P. Horne, L. A. Baker, Z. S. Siwy and C. R. Martin, *Langmuir*, 2006, **22**, 10837–10843.
20 J. Li, M. Gershow, D. Stein, E. Brandin and J. A. Golovchenko, *Nat. Mater.*, 2003, **2**, 611–615.
21 A. Mara, Z. Siwy, C. Trautmann, J. Wan and F. Kamme, *Nano Lett.*, 2004, **4**, 497–501.
22 L. J. Steinbock, O. Otto, C. Chimerel, J. Gornall and U. F. Keyser, *Nano Lett.*, 2010, **10**, 2493–2497.
23 A. J. Storm, J. H. Chen, H. W. Zandbergen and C. Dekker, *Phys. Rev. E: Stat., Nonlinear, Soft Matter Phys.*, 2005, **71**, 051903.
24 A. P. Ivanov, E. Instuli, C. M. McGilvery, G. Baldwin, D. W. McComb, T. Albrecht and J. B. Edel, *Nano Lett.*, 2011, **11**, 279–285.
25 A. Oukhaled, B. Cressiot, L. Bacri, M. Pastoriza-Gallego, J.-M. Betton, E. Bourhis, R. Jede, J. Gierak, L. Auvray and J. Pelta, *ACS Nano*, 2011, **5**, 3628–3638.
26 D. S. Talaga and J. Li, *J. Am. Chem. Soc.*, 2009, **131**, 9287–9297.
27 L. Movileanu, *Soft Matter*, 2008, **4**, 925–931.
28 Q. Zhao, J. Comer, V. Dimitrov, S. Yemenicioglu, A. Aksimentiev and G. Timp, *Nucleic Acids Res.*, 2008, **36**, 1532–1541.
29 B. McNally, M. Wanunu and A. Meller, *Nano Lett.*, 2008, **8**, 3418–3422.
30 B. Hornblower, A. Coombs, R. D. Whitaker, A. Kolomeisky, S. J. Picone, A. Meller and M. Akeson, *Nat. Methods*, 2007, **4**, 315–317.
31 C. Dekker, *Nat. Nanotechnol.*, 2007, **2**, 209–215.
32 C. Gao, S. Ding, Q. Tan and L.-Q. Gu, *Anal. Chem.*, 2009, **81**, 80–86.
33 O. V. Borisov, A. A. Darinskii and E. B. Zhulina, *Macromolecules*, 1995, **28**, 7180–7187.
34 P. G. de Gennes, *Adv. Polym. Sci.*, 1999, **138**, 91–105.
35 F. Jin and C. Wu, *Phys. Rev. Lett.*, 2006, **96**, 237801.
36 H. Ge, F. Jin, J. Li and C. Wu, *Macromolecules*, 2009, **42**, 4400–4402.
37 H. Ge, S. Pispas and C. Wu, *Polym. Chem.*, 2011, **2**, 1071–1076.
38 H. Ge and C. Wu, *Macromolecules*, 2010, **43**, 8711–8713.
39 L. Hong, F. Jin, J. Li, Y. Lu and C. Wu, *Macromolecules*, 2008, **41**, 8220–8224.
40 Q. Chen, H. Zhao, T. Ming, J. Wang and C. Wu, *J. Am. Chem. Soc.*, 2009, **131**, 16650–16651.
41 K. F. Freed and C. Wu, *J. Chem. Phys.*, 2011, **135**, 144902–144906.
42 K. F. Freed and C. Wu, *Macromolecules*, 2011, **44**, 9863–9866.
43 M. Wanunu, J. Sutin, B. McNally, A. Chow and A. Meller, *Biophys. J.*, 2008, **95**, 4716–4725.
44 G. M. Skinner, M. van den Hout, O. Broekmans, C. Dekker and N. H. Dekker, *Nano Lett.*, 2009, **9**, 2953–2960.
45 A. J. Storm, J. H. Chen, X. S. Ling, H. W. Zandbergen and C. Dekker, *Nat. Mater.*, 2003, **2**, 537–540.
46 A. V. Vologodskii, S. D. Levene, K. V. Klenin, M. Frank-kamenetskii and N. R. Cozzarelli, *J. Mol. Biol.*, 1992, 1224–1243.
47 R. Deng, Y. Yue, F. Jin, Y. C. Chen, H. F. Kung, M. C. M. Lin and C. Wu, *J. Controlled Release*, 2009, **140**, 40–46.
48 R. J. White, B. Zhang, S. Daniel, J. M. Tang, E. N. Ervin, P. S. Cremer and H. S. White, *Langmuir*, 2006, **22**, 10777–10783.
49 B. Zhang, J. Galusha, P. G. Shiozawa, G. Wang, A. J. Bergren, R. M. Jones, R. J. White, E. N. Ervin, C. C. Cauley and H. S. White, *Anal. Chem.*, 2007, **79**, 4778–4787.
50 B. Zhang, M. Wood and H. Lee, *Anal. Chem.*, 2009, **81**, 5541–5548.
51 O. Otto, L. J. Steinbock, D. W. Wong, J. L. Gornall and U. F. Keyser, *Rev. Sci. Instrum.*, 2011, **82**, 086102.
52 G. S. Manning, *Biopolymers*, 1981, **20**, 1751–1755.
53 D. Reguera, G. Schmid, P. S. Burada, J. M. Rubi, P. Reimann and P. Hanggi, *Phys. Rev. Lett.*, 2006, **96**, 130603.
54 S. E. Henrickson, M. Misakian, B. Robertson and J. J. Kasianowicz, *Phys. Rev. Lett.*, 2000, **85**, 3057–3060.
55 S. van Dorp, U. F. Keyser, N. H. Dekker, C. Dekker and S. G. Lemay, *Nat. Phys.*, 2009, **5**, 347–351.
56 U. F. Keyser, S. van Dorp and S. G. Lemay, *Chem. Soc. Rev.*, 2010, **39**, 939–947.
57 I. Teraoka, *Polymer Solutions: an Introduction to Physical Properties*, John Wiley & Sons, New York, 2002.
58 P.-G. de Gennes, *Scaling Concepts in Polymer Physics*, Cornell Press, New York, 1979.
59 T. T. Perkins, S. R. Quake, D. E. Smith and S. Chu, *Science*, 1994, **264**, 822–826.
60 T. R. Strick, J. F. Allemand, D. Bensimon, A. Bensimon and V. Croquette, *Science*, 1996, **271**, 1835–1837.
61 M. N. Dessinges, B. Maier, Y. Zhang, M. Peliti, D. Bensimon and V. Croquette, *Phys. Rev. Lett.*, 2002, **89**, 248102.
62 R. M. M. Smeets, U. F. Keyser, D. Krapf, M.-Y. Wu, N. H. Dekker and C. Dekker, *Nano Lett.*, 2006, **6**, 89–95.
63 D. A. Holden, G. Hendrickson, L. A. Lyon and H. S. White, *J. Phys. Chem. C*, 2011, **115**, 2999–3004.

